Hence they are not plotted separately. Figs. 3, 4 and 5 show the normalized $I(h)$–h curves for $N=20$ with $N=4$ for three different values of $N\varphi$, *viz.* 10, 20 and 30°.

$I(h)$–h curves in Fig. 1 show that for $N=20$ and $Q=\infty$, 36, 18 and 12 the maxima are slightly shifted in all cases and are no longer coincident with integral values of h. The maxima in the neighbourhood of $h=1$ are at $h=1{\cdot}02$ rather than at $h=1$ and those in the neighbourhood of $h=2$ are at $h=2{\cdot}02$ for all values of Q. The general features of all the curves are essentially same.

Fig. 2 shows that for $N=4$ and $Q=36$, 12, 6 and 4 the maximum in the neighbourhood of $h=1$ is at $h=1{\cdot}06$, $1{\cdot}075$, $1{\cdot}08$ and $1{\cdot}1$ respectively. The second maximum in the neighbourhood of $h=2$ is found to be at $h=2{\cdot}07$ for $Q=36$ and 12 whereas for $Q=6$ it is at $h=2{\cdot}10$ and for $Q=4$ at $h=2{\cdot}13$. The above two results show that the peak shifts become more appreciable as the value of Q decreases and also for the same value of Q as N decreases.

For $Q=1$ and $N=20$ it was observed in I that the intensity maximum in the neighbourhood of $h=1$ was at $h=1{\cdot}1$ rather than at $h=1$. For $N=10$ and $Q=2$ the maximum shifted to $h=1{\cdot}05$. It appears therefore, that the shift in maxima is a combined and complicated effect of the variation of N and φ.

Figs. 3, 4 and 5 show that the sharpness of the peaks for $N=20$ is more pronounced than that for $N=4$ for the same values of Q. Also it is observed from Fig. 1 that the intensity maxima and the broadening of the line profile remain almost the same for all values of Q. From Fig. 2 also similar observations can be made, but here the intensity maxima are less and the line profiles much broadened compared with Fig. 1. So from Figs. 1, 2, 3, 4 and 5 it can be concluded that the decrease in the value of N causes a decrease in the heights of maxima and broadens the line profile. This is an expected result as the decrease in the value of N is analogous to decrease in particle size. Further detailed numerical calculations for elucidating these points are being taken up.

References

BLACKMAN, M. (1951*a*). *Proc. Phys. Soc.* B **64**, 625.
BLACKMAN, M. (1951*b*). *Proc. Phys. Soc.* B **64**, 631.
BOWMAN, F. (1958). *Introduction to Bessel Functions*, p. 90. New York: Dover.
MITRA, G. B. (1965). *Acta Cryst.* **18**, 464.

Acta Cryst. (1968). A**24**, 269

X-ray Measurements of Stacking Faults in Copper–Antimony Alloys

BY M. DE AND S. P. SEN GUPTA,

Department of General Physics and X-rays, Indian Association for the Cultivation of Science, Calcutta-32, India

(*Received* 6 *June* 1967)

The line profiles from cold-worked copper-base alloys containing pentavalent solute antimony in the primary solid solution range have been recorded by a Geiger counter X-ray diffractometer. The deformation fault probability α and the twin fault probability β have been obtained from peak shift and peak asymmetry measurements respectively. A roughly parabolic variation of α with increasing solute content has been observed. However, the increase of α with the increase of solute valency for fixed electron concentration per atom is not clearly established. The twin fault probability β also increases in a similar way as observed in other copper-base alloys.

During recent years extensive studies have been made of the presence and effects of stacking faults in copper- and silver-base alloys containing di-, tri- or tetravalent solutes and measurements with pentavalent solutes have been lacking. Recently, Sastry, Rama Rao & Anantharaman (1966) and Sen Gupta (1967) have determined the stacking fault concentrations in alloys of silver with the pentavalent solute antimony and observed the possible correlations between stacking fault probability α and the solute valence as well as electron concentration per atom, e/a. The present note reports results of our X-ray measurements of deformation and twin stacking fault probabilities α and β from peak shift and peak asymmetry in cold-worked copper–antimony alloys in the solid solution range.

Alloys were prepared from spectrographically standardized copper and antimony supplied by Messrs Johnson, Matthey & Co., Ltd, London, following the same method as adopted previously (Sen Gupta & Quader, 1966), the homogenization temperature being 650–750 °C. The annealing treatments were terminated by quenching in water. Weight changes during preparation were negligible and hence no chemical analyses of the alloy specimens were performed. Preparations of the cold-worked and annealed samples and recordings of the line profiles of several X-ray reflexions were carried out in the usual way (Sen Gupta & Quader, 1966). Cold-working and the experimental observations were done at room temperature, 30 ± 1 °C. No phase transformation has been observed due to cold work.

The deformation fault probability α was obtained from the neighbouring pairs of 111–200, 200–220 and 220–311 reflexions by use of the relation (Wagner, 1957):

$$(2\theta^0_{hkl}-2\theta^0_{h'k'l'})_{CW}-(2\theta^0_{hkl}-2\theta^0_{h'k'l'})_{Ann}=H\,.\,\alpha \qquad (1)$$

and

$$H=(\langle G\rangle j\,.\,\tan\theta^0)_{hkl}-(\langle G\rangle j\,.\,\tan\theta^0)_{h'k'l'}\,, \qquad (2)$$

where the parameters $\langle G\rangle$ and j have their usual meanings. The peak positions were obtained from midpoints by extrapolation to the peak maximum. The estimated accuracy in 2θ of the determination of the peak maximum position is about $\pm 0{\cdot}01°$ for 2θ less than 75° and $\pm 0{\cdot}02°$ for 2θ of larger values.

The twin fault probability β was obtained in a similar way to that adopted earlier (Sen Gupta & Quader, 1966), *i.e.* from the displacements of the centre of gravity of cold-worked 111 and 200 peaks using the relation (Cohen & Wagner, 1962):

$$\beta=\frac{\Delta C\,.\,G\,.\,(^0 2\theta)_{111}-\Delta C\,.\,G\,.\,(^0 2\theta)_{200}}{11\tan\theta_{111}+14{\cdot}6\tan\theta_{200}\,.} \qquad (3)$$

Table 1 summarizes the values of β and the average values of α for the five compositions of Cu–Sb and Figs. 1 and 2 show the variation of α with solute content and electron concentration respectively for Cu–Sb alloys together with Cu–In and Cu–Sn alloys (Goswami, Sen Gupta & Quader, 1966). Variation of β with solute content has also been shown in Fig. 1.

It is apparent from Table 1 that in general the values of α computed from the change in separations of the 220–200 peaks are higher whereas those from 200–111 peaks are less and there is a fair agreement for the three sets. The deformation fault probability α has been found to increase with increasing solute content in a similar way to that observed in Cu–In and Cu–Sn alloys (Fig. 1), and for a fixed amount of solute present α is higher in this system as compared with others, as has also been observed for silver-base alloys (Adler & Wagner, 1962; Sen Gupta, 1967). It may be noted that the variation of α with increasing solute content is linear for silver-base alloys and roughly parabolic for copper-base alloys. From Fig. 2, it is clear that α increases with electron concentration. But the increase of fault probability α with the increase of solute valency for fixed e/a is not clearly established here, although

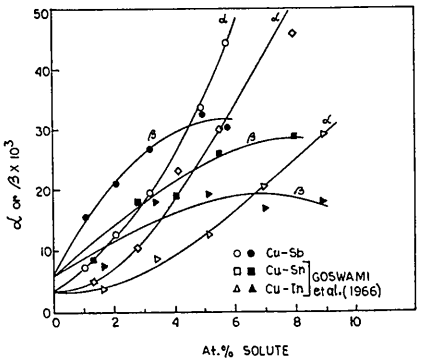

Fig. 1. Deformation and twin fault probability α and β as a function of solute concentration in copper-base alloys.

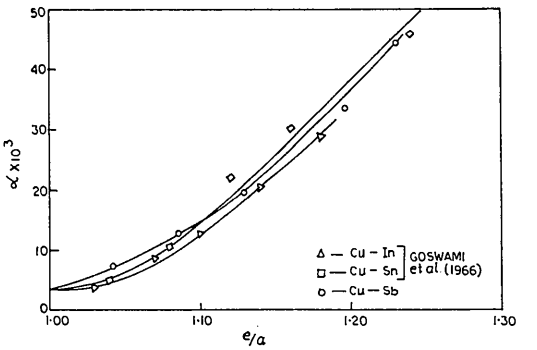

Fig. 2. Deformation fault probability α as a function of electron concentration in copper-base alloys.

Table 1. *Stacking fault probability α and β for copper–antimony alloys*

Composition (at. %)	*hkl*	*h'k'l'*	$\Delta(2\theta_{hkl}-2\theta_{h'k'l'})$	$\alpha\times10^3$	$\langle\alpha\rangle\times10^3$	$\Delta\Delta$ C.G.*	$\beta\times10^3$
Cu – 1·05 Sb	200	111	−0·040°	7·58			
	220	200	+0·045	6·73	7·42	+0·175°	15·62
	311	220	−0·035	7·95			
Cu – 2·10 Sb	200	111	−0·045	8·56			
	220	200	+0·085	12·77	12·59	+0·236	21·13
	311	220	−0·072	16·43			
Cu – 3·23 Sb	200	111	−0·074	14·15			
	220	200	+0·155	23·42	19·42	+0·297	26·71
	311	220	−0·090	20·68			
Cu – 4·88 Sb	200	111	−0·155	29·77			
	220	200	+0·255	38·74	33·48	+0·361	32·61
	311	220	−0·138	31·94			
Cu – 5·79 Sb	200	111	−0·205	39·50			
	220	200	+0·330	50·32	44·28	+0·334	30·27
	311	220	−0·185	43·01			

* $\Delta\Delta$ C.G. = Δ C.G. $(^\circ 2\theta)_{111}-\Delta$ C.G. $(^\circ 2\theta)_{200}$

this has been previously observed in some copper- and silver-base alloys (Davies & Cahn, 1962; Adler & Wagner, 1962; Goswami *et al.*, 1966; Sen Gupta, 1967). However, it may be mentioned that the fault probability α has been obtained from neighbouring pairs of reflexions and the average value of α has been considered in the present case, whereas in the earlier measurements of α for Cu–In, Cu–Sn alloys (Goswami *et al.*, 1966) only the first pair of reflexions were considered.

The twin fault probability β also increases with increasing solute content (Fig. 1) and it is observed that apart from the limitations which exist in the determination of β (Sen Gupta & Quader, 1966), the trend of variation is similar in all cases attaining saturation at higher solute content, and for a fixed amount of solute present β also increases in the order Cu–In, Cu–Sn, Cu–Sb.

The authors are grateful to Prof. B. N. Srivastava, D.Sc., F.N.I., for his keen interest in the work and to the Council for Scientific and Industrial Research (New Delhi) for financial assistance.

References

ADLER, R. P. I. & WAGNER, C. N. J. (1962). *J. Appl. Phys.* **33**, 3451.
COHEN, J. B. & WAGNER, C. N. J. (1962). *J. Appl. Phys.* **33**, 2073.
DAVIES, R. G. & CAHN, R. W. (1962). *Acta Metallurg.* **10**, 621.
GOSWAMI, K. N., SEN GUPTA, S. P. & QUADER, M. A. (1966). *Acta Cryst.* **21**, 243.
SASTRY, D. H., RAMA RAO, P. & ANANTHARAMAN, T. R. (1966). *Trans. AIME*, **236**, 1291.
SEN GUPTA, S. P. & QUADER, M. A. (1966). *Acta Cryst.* **20**, 798.
SEN GUPTA, S. P. (1967). *Acta Cryst.* **23**, 244.
WAGNER, C. N. J. (1957). *Acta Metallurg.* **5**, 427.

Acta Cryst. (1968). A**24**, 271

Crystal Setting by Rotation Photographs

BY R. J. DAVIS
Department of Mineralogy, British Museum (Natural History), Cromwell Road, London, S.W.7, England

(*Received* 19 *April* 1967)

Applications are described of a simplification and generalization of Roof's method of setting single crystals by rotation photographs. The method is particularly recommended for setting irregular fragments of known unit cell to a specified axis.

Roof (1955) has described a method of setting triclinic crystals to a zone axis by taking three trial rotation photographs, making shifts $\delta\alpha°$, $\delta\beta°$ on the two goniometer arcs in turn between exposures. If $\delta\alpha$ and $\delta\beta$ are reasonably small, equivalent reflexions can be recognized on the three photographs. By selecting two prominent low-angle reflexions near the equator, measuring their departures from the equator as $\tan N=\zeta/\xi$ in each of the six cases, and using the nomogram given by Roof, one derives arc corrections which bring the two reflexions onto the equator exactly, and thus to coincide with their equivalent reflexions previously below the equator. The crystal is then set to a zone axis, and if the two reflexions were properly selected initially, the axis will probably be a prominent one.

Roof's method has now been superseded by that of Brooker & Nuffield (1966) who use a similar triplet of rotation photographs, but taken in a flat-film camera; they show how one may transfer data for any number of recorded reflexions to a stereogram of the crystal in its random setting, from which one may deduce symmetry if any, and more reliable positions for the main zone axes. Their method is relatively laborious, however, and I have found the following simplification and generalization of Roof's method useful on several occasions.

Theoretical

The method depends on the essentially empirical observation that if the separation between a pair of equivalent reflexions is measured with a ruler, then to a good approximation it plots as a plane on a square mesh of α and β, the goniometer arc readings.

Consider the crystal in terms of spherical polar coordinates on the required zone axis as origin. The planes giving rise to the (coincident) spots on the rotation photograph are then at (φ,ϱ), $(-\varphi,\varrho)$ respectively. If the crystal is rotated to some other rotation axis, having coordinates (φ',ϱ') on this coordinate system, the planes now have ϱ-values, ϱ_1,ϱ_2, given by:

$$\cos\varrho_1=\cos\varrho\cos\varrho'+\sin\varrho\sin\varrho'\cos(\varphi'+\varphi)$$
$$\cos\varrho_2=\cos\varrho\cos\varrho'+\sin\varrho\sin\varrho'\cos(\varphi'-\varphi).$$

Subtracting:

$$2\sin\tfrac{1}{2}(\varrho_1+\varrho_2)\sin\tfrac{1}{2}(\varrho_1-\varrho_2)=2\sin\varrho\sin\varrho'\sin\varphi\sin\varphi'.$$

Rotations of the crystal in the direction $\varphi'=0°$ or $180°$